JOURNAL OF GUIDANCE, CONTROL, AND DYNAMICS
Vol. 24, No. 1, January–February 2001

Computational Fluid Dynamics and Doublet-Lattice Calculation of Unsteady Control Surface Aerodynamics

K. M. Roughen,* M. L. Baker,† and T. Fogarty‡
The Boeing Company, Long Beach, California 90807

Accurate prediction of control surface aerodynamics has been a challenge since the dawn of aviation. Whereas this has been an important problem for many years, recent increases in the use of control surfaces for active control (load alleviation and flutter suppression) have increased the importance of accurate steady and unsteady control surface aerodynamics. Because of the strong influence of viscosity on the pressures on a trailing-edge control surface, the aerodynamic theories based on the linear potential equation have had only marginal success in predicting control surface aerodynamics, and in practice, large corrections (based on wind-tunnel data) are often required for acceptable accuracy. Recent advances in computing technology and unsteady aerodynamic codes based on the Navier–Stokes equation are allowing more accurate analyses to be performed. Unsteady aerodynamic calculations due to control surface oscillations are made using a linear potential code (N5K) and a Navier–Stokes code (CFL3D.AE-BA version 4.1). The Navier–Stokes calculations are performed in the time domain using an exponential pulse technique and are transformed to the frequency domain using Fourier transform. For low reduced-frequency cases, the Navier–Stokes calculations are compared to the doublet-lattice method and to experiment, and the advantages of the nonlinear analysis are clearly demonstrated. Correlation between Navier–Stokes and doublet-lattice results is then studied for higher reduced frequencies.

Introduction

WITH the increased interaction among the aerodynamic, structures, and controls disciplines in advanced aircraft, it is increasingly important to predict accurately the aerodynamic forces due to control surface deflection. The aerodynamic behavior of oscillating control surfaces has historically been difficult to predict analytically. The doublet-lattice method (DLM)[1] has been the de facto standard unsteady aerodynamic analysis tool in the subsonic regime for decades, but because it is based on the linear potential equation, it has had limited success in computing control surface aerodynamics. In practice, the aerodynamic results from the DLM (or a similar process) were modified using (sometimes large) correction factors to improve correlation with test data. These correction factors are typically based on steady wind-tunnel data and are applied to steady and unsteady conditions alike. This is undesirable because the steady corrections will not necessarily be representative of the unsteady flow and cannot correct the unsteady phase lag.

With the advent of low-cost, high-power computers, the use of unsteady computational fluid dynamics (CFD) for the calculation of unsteady control surface aerodynamics has recently become more attractive. In this study, CFL3D.AE-BA[2] was used to compute unsteady Navier–Stokes solutions of oscillatory control surface motion. This model includes not only the effects of compressibility and transonic shocks, but also accounts for viscous effects. To reduce the computational time of the CFD solutions, the control surface deflection (as a function of time) has the form of an exponential pulse (as opposed to a pure sinusoid), and the frequency-domain unsteady aerodynamics were computed using a Fourier transform.

For cases with small angle of attack and no deflected control surface, linear lifting surface theory has been shown to be valid outside the transonic regime. This approach is no longer valid when analysis is required for cases involving transonic flow or significant viscous effects, or when modeling of details such as control surface gaps is important. Upstream propagation of information for cases in the transonic regime also cannot be predicted by linear theory. A classic example of such flow characteristics occurs in the shock wave present for flows with a supersonic pocket at the surface of the wing. There is a significant difference in the magnitude and phase results obtained from linear theory and those obtained from test and CFD in the region upstream of the transition back to subsonic flow. It is the purpose of this study to investigate the benefits of higher fidelity aerodynamic theories in improving the accuracy of unsteady aerodynamic predictions.

Wind-Tunnel Model

To evaluate the accuracy of our analytical methods, it was necessary to compare them with test data. For this study, the Benchmark Active Controls Technology[3,6–9] (BACT) wing was used (Fig. 2 in Ref. 4). The BACT model was tested in the Transonic Dynamics Tunnel (TDT) at NASA Langley Research Center. The model is a rectangular wing with NACA 0012 symmetric airfoil shape. The model has a trailing-edge control surface extending from 45 to 75% span. The control surface hingeline is located at the 75% chord station. For testing purposes unrelated to our study, upper and lower surface spoilers were added with hingelines at the 60% chord station with the same spanwise dimensions and locations as the trailing-edge control surface. Testing of the wing was conducted using Freon (R-12) as the flow medium. For the steady-state tests, the mean pressure measurements were available. For the unsteady-state tests, the time history of the pressures were available and were converted to the frequency domain using a Fourier transform. This yielded the pressure in terms of the response in phase with the flap motion (real) and 90 deg out of phase from the flap motion (imaginary). A simple calculation was used to convert this information to magnitude and phase.

Pressures were measured at the 40 and 60% span locations. This study concentrates on the data collected at the 60% span location, which is the center of the trailing-edge control surface. There are 58 pressure orifices at this span location.

Correlation of CFD to test data for the BACT model was accomplished by Schuster et al.[5] with a ENS3DAE Navier–Stokes analysis. In the investigation discussed in this paper, the first step was to validate CFL3D similarly. The study performed by Schuster et al. was used as another source of comparison for the validity of our CFD results.

Presented as Paper 99-1469 at the AIAA/ASME/ASCE/AHS/ASC 40th Structures, Structural Dynamics, and Materials Conference and Exhibit, St. Louis, MO, 12–15 April 1999; received 28 May 1999; revision received 3 January 2000; accepted for publication 3 March 2000.

*Engineer/Scientist, Phantom Works Loads and Dynamics.
†Manager, Phantom Works Loads and Dynamics. Member AIAA.
‡Senior Engineer/Scientist, Phantom Works Loads and Dynamics.

Analytical Models

For the analysis performed in this study, doublet-lattice and Navier–Stokes models were required. Theoretical geometry of the NACA 0012 airfoil was used to create the analytical models. Because the BACT wing configuration is so simple, the DLM model consisted of a single panel broken down into 15 spanwise strips and 36 chordwise boxes. Based on the criteria in Ref. 1, this is expected to be valid up to a reduced frequency of $k_r = 2.0$.

For the Navier–Stokes solutions, a three-dimensional volume grid was required. A baseline C–H topology grid was obtained from the authors of Ref. 4. Changes were made to add gaps, increase resolution in the boundary layer, and increase resolution at the trailing edge. Because overall computer resources were limited, this resulted in sacrificing streamwise grid clustering near the hingeline. As will be observed, the resolution of this grid was not sufficient to capture all of the details of the unsteady aerodynamics (particularly at the hingeline), but most of the correlation with the experimental results was admirable. The final grid had 557,685 grid points ($153 \times 81 \times 45$) and is shown in Fig. 1.

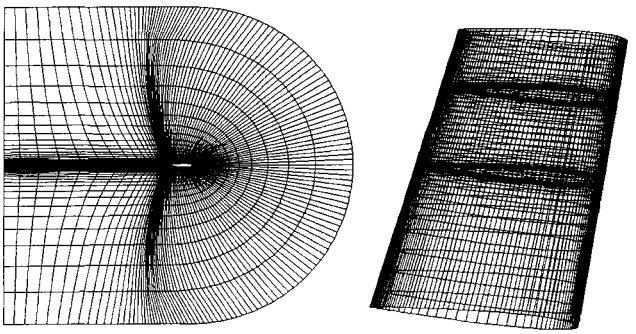

Fig. 1 CFL3D $153 \times 81 \times 45$ grid.

Process

For the results discussed in this study, the CFD runs were performed with an exponential pulse input. This was done to economize computer time because fewer runs are needed for analysis using a pulse as compared to a sinusoidal input. This is due to the ability to convert to the frequency domain at multiple frequencies from a single run when using the pulse technique. It is our experience that good accuracy can be obtained using pulse input if care is taken to ensure that the simulation is sufficiently long that the transients die out. This usually requires shorter time histories than a harmonic

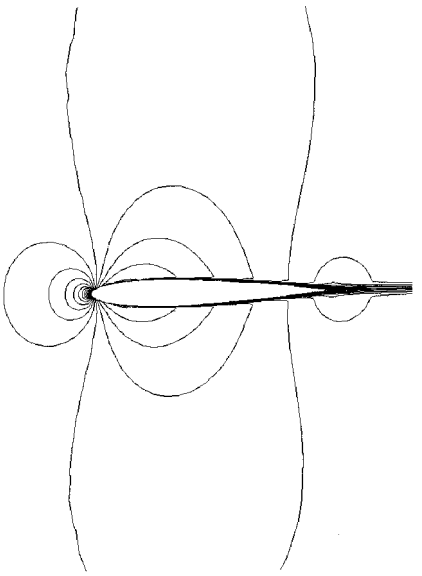

Fig. 4 Mach contours for $M_\infty = 0.65$.

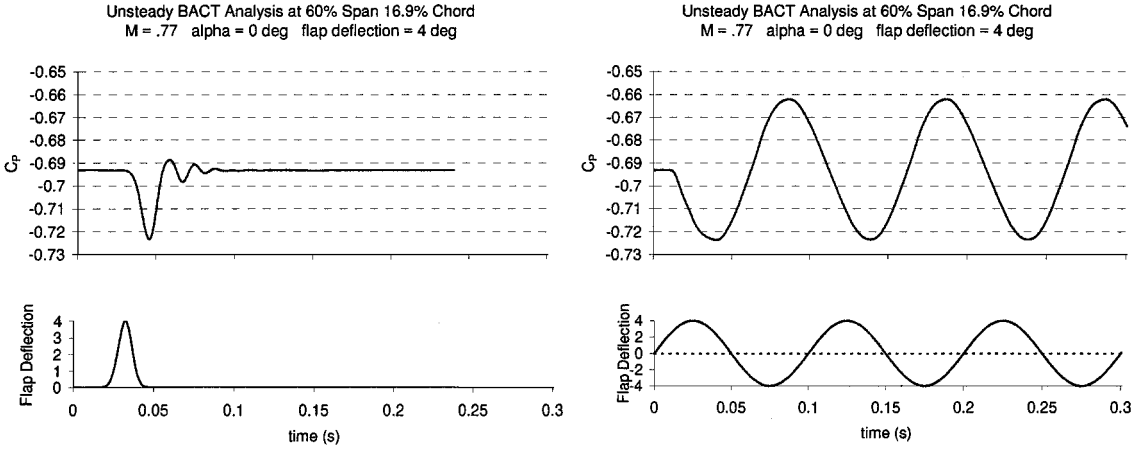

Fig. 2 Time history results from CFL3D.

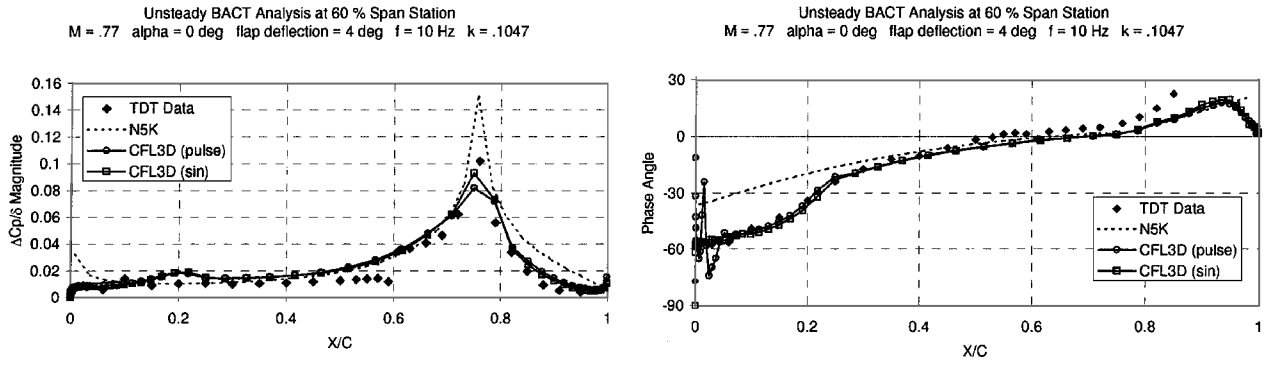

Fig. 3 Unsteady pressure coefficient comparison between pulse and sinusoidal input.

solution of three cycles (which was our standard for harmonic solutions), especially at low frequencies. Sample time history pressure results are shown for both types of input at one location on the wing for the Mach 0.77 case (Fig. 2).

It is recognized that this approach is only an approximation for truly nonlinear flows because the Fourier transform approach assumes linearity. However, comparison between results from the transformed pulse input and the more conventional sinusoidal

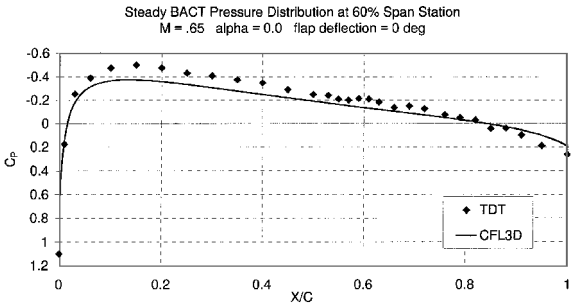

Fig. 5 Steady pressure coefficient for $M_\infty = 0.65$.

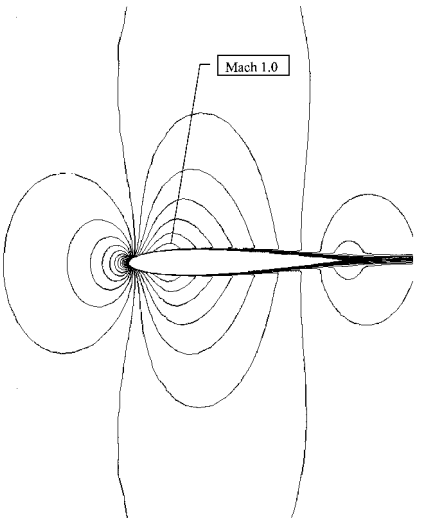

Fig. 7 Mach contours for $M_\infty = 0.77$.

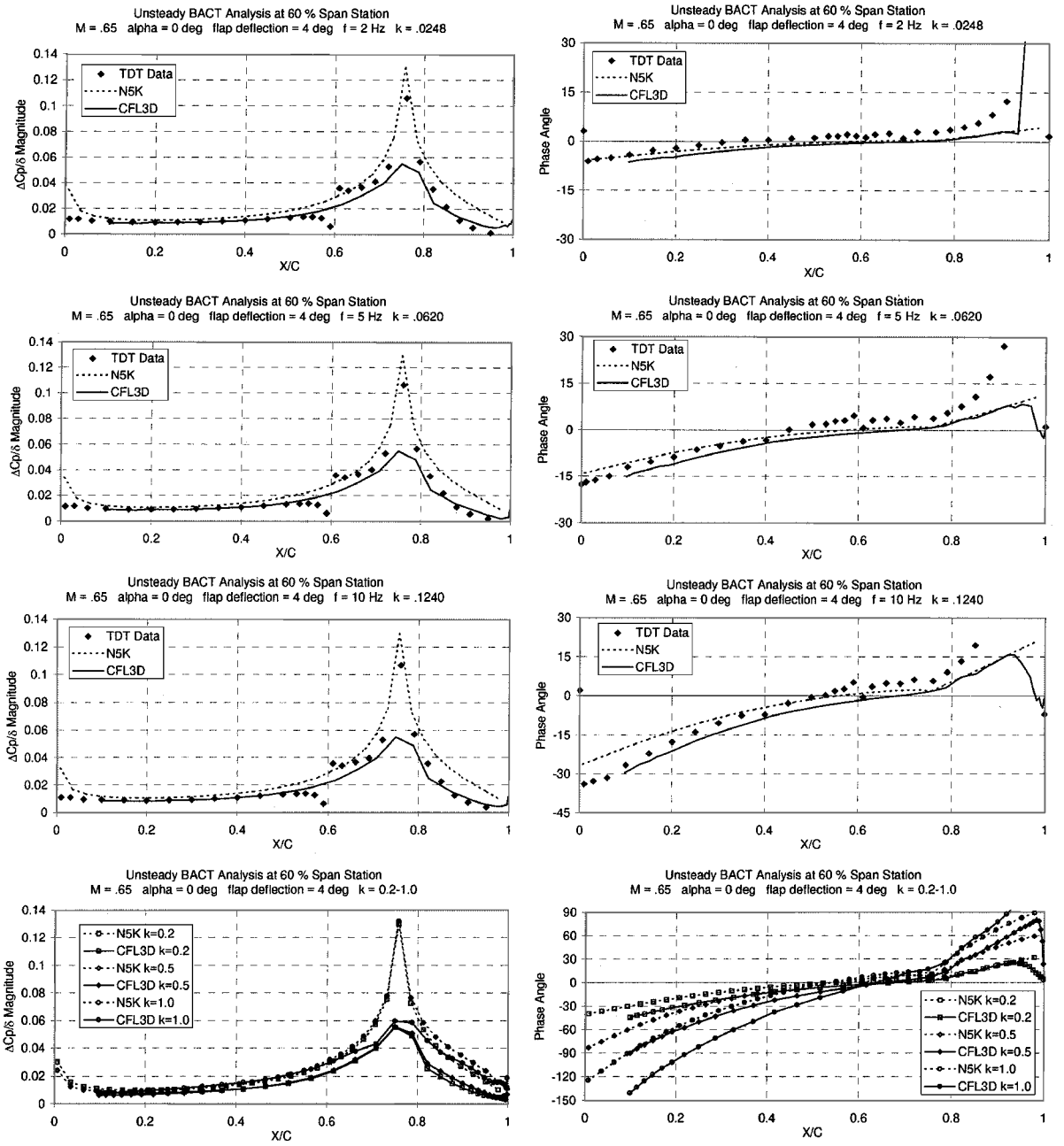

Fig. 6 Unsteady pressure coefficient for reduced frequency from 0.0248 to 1.0.

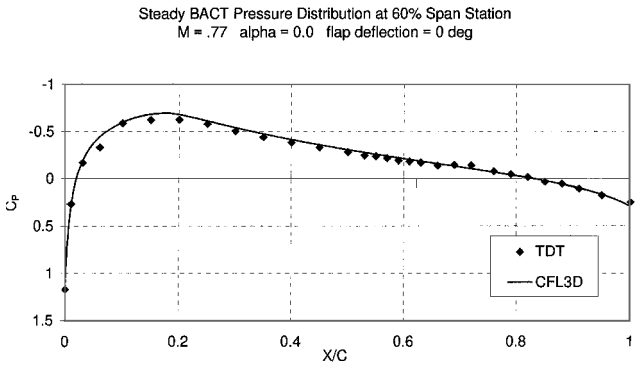

Fig. 8 Steady pressure coefficient for $M_\infty = 0.77$.

input indicate that this approach is sufficiently accurate to justify the savings in computer time.

To examine the validity of the pulse input method, a case was analyzed using both pulse and harmonic control surface inputs for CFL3D. The results are shown in Fig. 3. The run with pulsed input correlates acceptably well with the run with sinusoidal input. The magnitude results from the pulse run are almost identical to the results from the pulse run except for a single grid point at the hinge line. The phase results from the pulse run show noise toward the leading edge, which was not present in the results from the sinusoidal run. Because of the presence of noise near the leading edge of the run performed with pulse input, the CFD results at the leading edge are not shown in plots elsewhere in this paper. To obtain acceptable results near the leading edge, sinusoidal runs would need to be performed for all cases. Because the magnitude of the unsteady

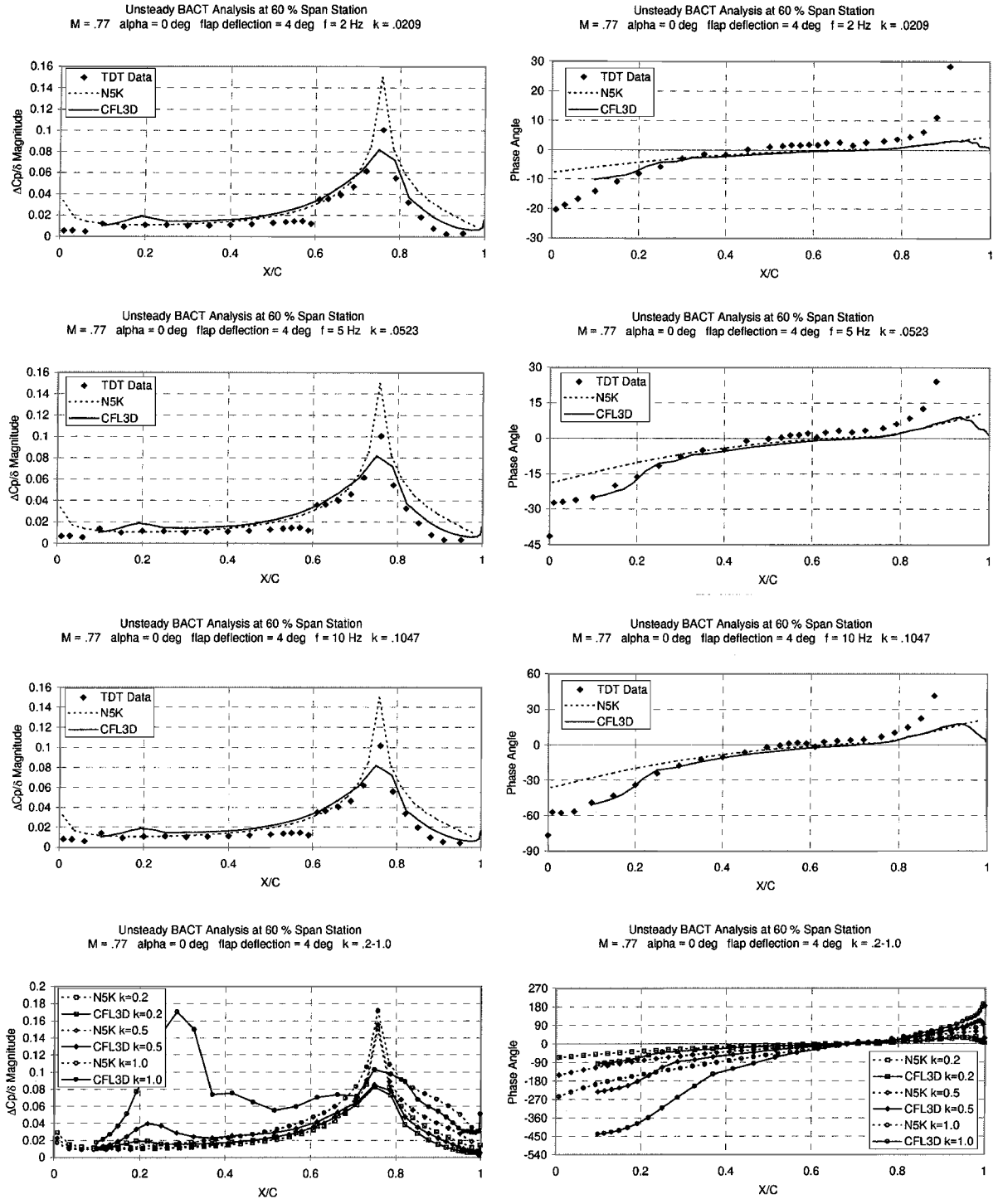

Fig. 9 Unsteady pressure coefficient for reduced frequency from 0.0209 to 1.0.

pressure is small at the leading edge, the noise in the phase angle is of little importance and the increase of accuracy gained by performing sinusoidal runs for all cases would be predominantly aesthetic.

Results

Steady-State Results

The results obtained from the steady-state runs of CFL3D are presented for all Mach numbers studied. These results have been plotted along with test data. Because the cases run were symmetric with zero angle of attack, the experimental data for the upper and lower surface were averaged to obtain a result for one surface. The Mach 0.65 case is shown to be purely subsonic by its Mach contour plot (Fig. 4). The steady-state pressure data for the Mach 0.65 run agrees reasonably well with the test data as shown in Fig. 5. The unsteady pressure coefficient for several reduced frequencies is shown in Fig. 6. In the Mach contour plot for the Mach 0.77 case (Fig. 7), smooth transitions to and from a supersonic region are present. As in the purely subsonic case, the pressure results are in agreement with the test data (Fig. 8). Unsteady pressure coefficients are shown in Figs. 9 and 10. There is a clear shock downstream of the supersonic region in the Mach 0.82 case (Fig. 11). The pressure results show reasonable agreement with test data except in the region of the shock, where the pressure discontinuity is predicted to be slightly larger and farther aft than is seen in the test data (Fig. 12).

Unsteady Results with Pulsed Aileron

This study concentrated on zero-angle-of-attack cases ranging from a frequency of 2 Hz to a reduced frequency of 1.0. The Mach numbers studied range from $M = 0.65$ to 0.82. Several observations can be made from the results shown in Figs. 4–13.

Mach 0.65

For the purely subsonic condition shown in Figs. 4–6 (Mach 0.65), there is relatively good agreement between the doublet-lattice results, the Navier–Stokes results, and the test data. This is not surprising because the flow is entirely subsonic and well behaved (Fig. 4). The magnitude of the unsteady pressure as computed by the DLM is fairly close to the experimental results over much of the chord, but there are areas where the DLM clearly does not contain the relevant physics. The most obvious is the peak in unsteady pressures at the leading edge, which is absent from the experimental data. The results of the pulse-deflection Navier–Stokes analysis near the leading edge were omitted due to the noise in the results, as described earlier. The pressure distribution on the flap itself (aft of the hingeline) also shows significant deviation from the experimental results. One area of surprisingly good correlation between doublet-lattice and wind-tunnel results is the unsteady pressure at and immediately forward of the hingeline itself. The prediction of the unsteady pressure phase angle from DLM is also fairly good, but deviates from the experimental results aft of the control surface hingeline.

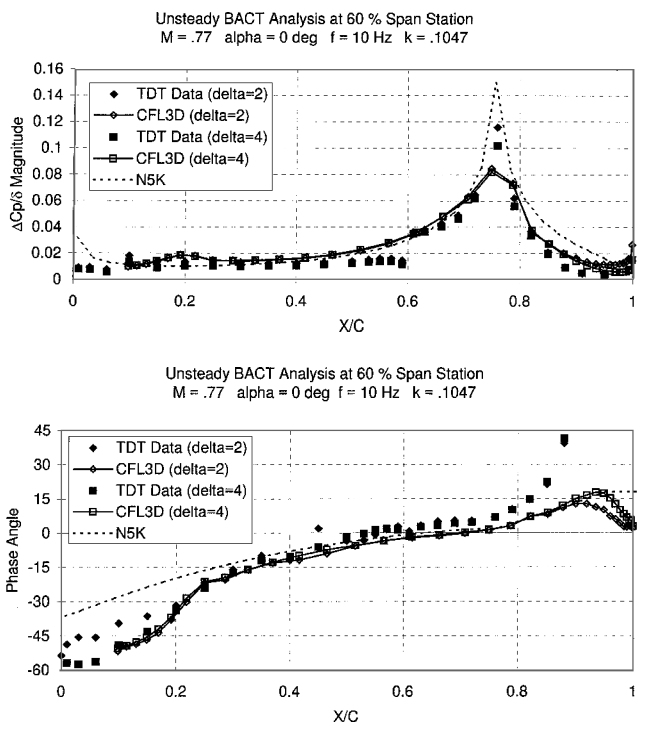

Fig. 10 Unsteady pressure coefficient for flap deflection of 2 and 4 deg for $M_\infty = 0.77$ and $f = 10$ Hz.

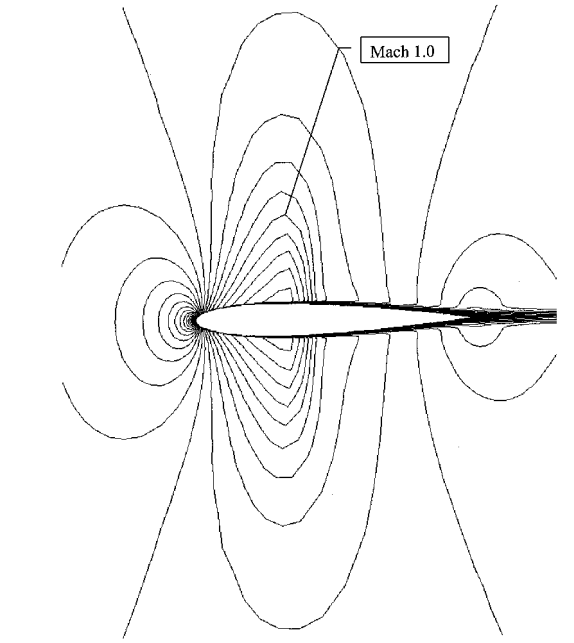

Fig. 11 Mach contours for $M_\infty = 0.82$.

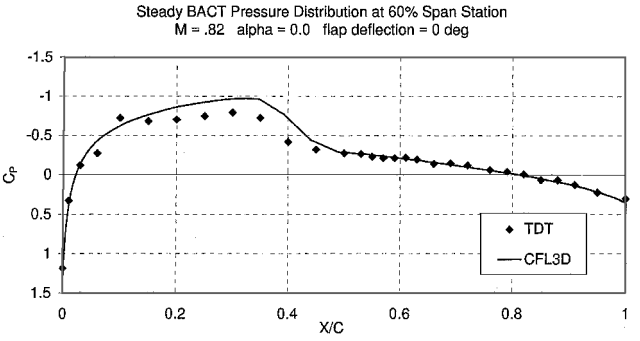

Fig. 12 Steady pressure coefficient for $M_\infty = 0.82$.

The Navier–Stokes results, as expected, show somewhat better correlation with the test data. The use of the pulse method prevents demonstrating the absence of the leading-edge peak in unsteady pressure that was seen in the doublet-lattice results; however, this peak is absent in the sinusoidal Navier–Stokes solution for the Mach 0.77 case shown in Fig. 3. The pressure magnitude distribution on the flap itself is much closer to the experimental results than the DLM, and the pressures on the airfoil forward of the hingeline are in excellent agreement with the experimental data. The correlation of the unsteady pressure peak at the hingeline itself is disappointing, however, with the Navier–Stokes results showing significantly lower peaks than the test data. This is due to a relatively coarse CFD mesh in the chordwise direction in the vicinity of the hingeline. The correlation of the unsteady phase angle is similar to the doublet-lattice results. There is good agreement with the experiment except on the flap itself. Because the magnitude of the unsteady pressures is so small in this region, this represents a relatively minor inaccuracy, and it is not certain that the experimental results are meaningful.

At higher reduced frequencies, the discrepancies between the unsteady pressure magnitudes seen in the doublet-lattice and Navier–Stokes results are seen to diminish until, at a reduced frequency

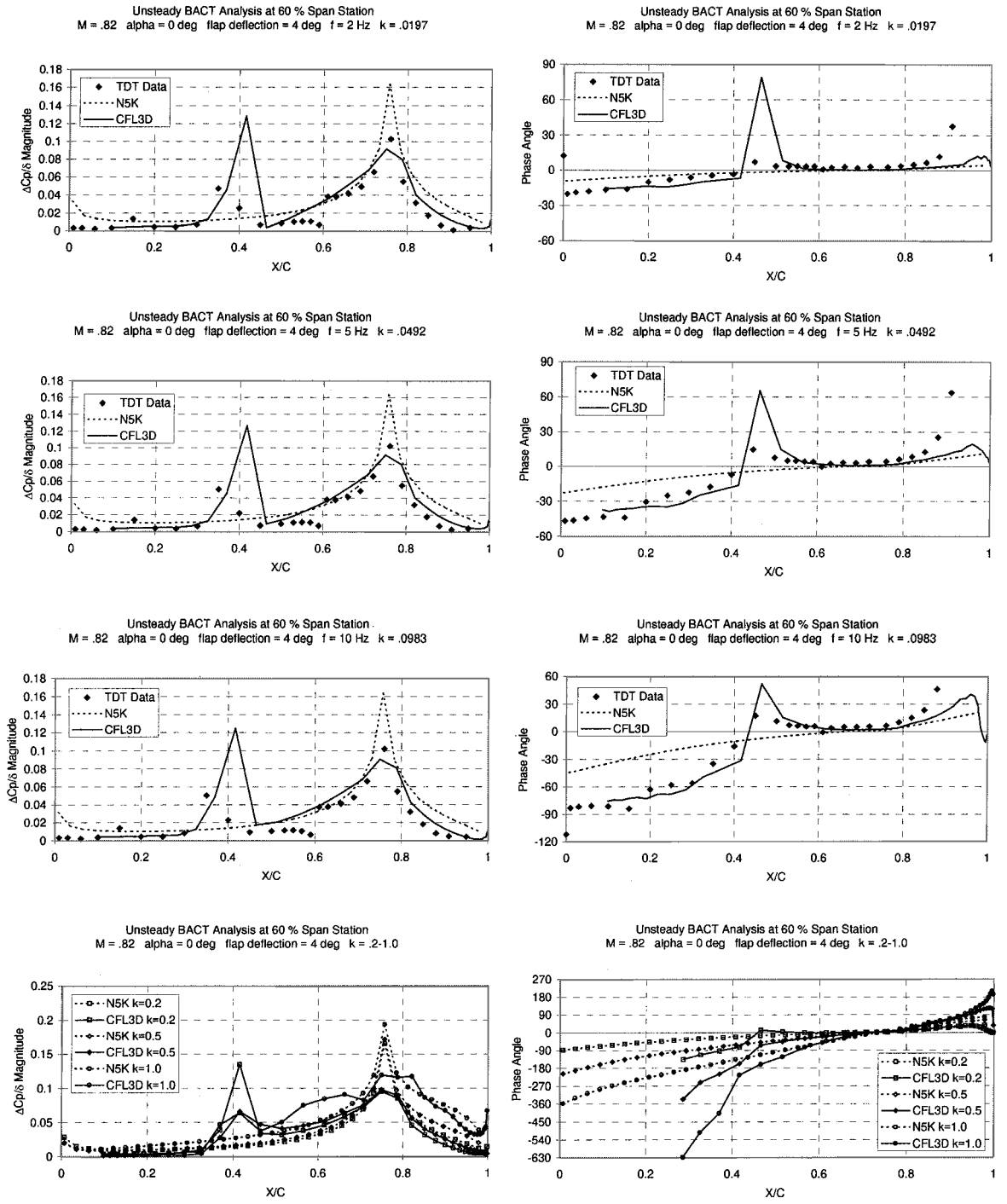

Fig. 13 Unsteady pressure coefficient for reduced frequency from 0.0197 to 1.0.

of $k = 1.0$, there is almost no difference except at the hingeline. The results show increasing discrepancies in the phase angle of the unsteady pressures with higher reduced frequencies.

Mach 0.77

Transonic effects begin to become apparent in these results. For the most part, the observations about the results and the qualitative correlation between doublet-lattice, Navier–Stokes, and experimental results are similar to the subsonic results. However, there are some important differences that appear in the neighborhood of the supersonic pocket. Figure 7 shows Mach contours of the steady-state solution in the plane of the pressure measurements. The region from approximately 10–25% chord has supersonic flow, but the downstream termination of the supersonic region is a gentle recompression, rather than a shock. However, the flow being locally supersonic causes a significant change in the upstream propagation of information. This is most clearly seen in the unsteady pressure phase plots in Fig. 9. Whereas in the subsonic case, the phase shows a fairly linear variation upstream of the hingeline (governed by upstream propagation of information), the Mach 0.77 results clearly show nonlinear behavior. There is an inflection point in the phase-vs-chord plots at approximately 25% chord. This roughly corresponds to the location where an upstream-traveling signal would encounter supersonic flow. The signal must, in effect, travel around the supersonic region to influence surface pressures, which causes an increased phase lag. This results in a steeper slope in the phase-vs-chord curve in the supersonic region. This gradually levels out near the leading edge, where the flow is again subsonic. There is excellent qualitative agreement between the experimental and Navier–Stokes results in this area.

The effect of the supersonic pocket can also be seen in the magnitude plots of the Navier–Stokes results. There is clearly a bump in the unsteady pressure magnitude at approximately 20% chord, which corresponds to the recompression region. Behavior aft of the

hingeline is similar to that seen in the subsonic case, with the Navier–Stokes results showing better magnitude results than the DLM.

The effects of increasing the amplitude of the unsteady flap motion can be seen in Fig. 10. In these analyses, the flap motion had a maximum amplitude of 4 deg. Little nonlinear amplitude dependence is seen except near the trailing edge.

Mach 0.82

The steady Mach contours in Fig. 11 show the presence of a transonic shock at approximately 40% chord in the Mach 0.82 case. The presence of the shock is also clearly evident in the steady-state pressure distribution shown in Fig. 12. The effects of the shock are also quite obvious in the unsteady pressure results. In the unsteady pressure magnitudes, there is a clear peak in the unsteady pressure at approximately 35% local chord in the experimental results and at 40% local chord in the Navier–Stokes results. The peak, which represents the shock doublet caused by unsteady chordwise motion of the shock, is absent in the linear doublet-lattice results. Quantitatively, the correlation of the shock doublet peak between experimental and Navier–Stokes results is disappointing. The CFD results predict a shock doublet of approximately double the amplitude of that seen in the experimental results. This indicates that the shock in the CFD solution is somewhat stronger than that found in the experiment. Two possible contributors to this inaccuracy are the chordwise grid resolution and the Baldwin–Lomax turbulence model used in this study.

A similar phenomenon is seen in the phase angle of the unsteady pressures. There is a clear discontinuity in the phase angle across the shock in both the experiment and the Navier–Stokes analysis. However, the magnitude of the discontinuity in the Navier–Stokes solution is significantly larger than that seen in the experiment. Note that the phase results upstream of the shock were not included in the Navier–Stokes results because low-pressure magnitude in this region creates numerical problems due to roundoff error.

Correlation between the CFD solutions and the experiment is excellent away from the neighborhood of the shock. Forward of the shock, both the CFD and the experiment show almost no unsteady pressure fluctuations due to the large supersonic region. Aft of the shock, the magnitude correlation is excellent, including the peak at the hinge line and the pressures on the flap itself. Consistent with the other Mach numbers, the phase of the experimental pressures on the flap does not agree with the analysis, but this is not very significant due to the extremely low-pressure magnitudes in this region.

Conclusions

Unsteady aerodynamic analysis has been performed using a linear lifting surface code (N5K) and a Navier–Stokes code (CFL3D.AE-BA) for cases with varied Mach number and frequency. Inaccuracies in the doublet-lattice results are clearly seen in regions where linear potential theory is not valid, whereas the results of the CFD analyses demonstrate good correlation with test data. Throughout this paper, an exponential pulse technique was used to compute frequency-domain aerodynamics from the Navier–Stokes simulations. Comparison of this technique with a more conventional sinusoidal input shows excellent accuracy away from the leading edge, where unsteady pressure magnitudes are small.

Correlation with CFD and test data demonstrates the limits of accuracy for the DLM. The magnitude results obtained from linear theory are acceptable except on the control surface, toward the leading edge, and near and upstream of transonic shocks. This is in agreement with theory, as viscous effects are relevant on the control surface, thickness effects are relevant toward the leading edge, and transonic effects are relevant in cases with shocks. None of these effects are accounted for in linear potential flow. The magnitude results on the flap obtained from the DLM are consistently too high when compared to CFD and test data. The results for magnitude are also consistently too large near the leading edge. This results in overprediction of lift and hinge moments. The unsteady pressure magnitude and phase in the neighborhood of supersonic regions are inaccurate, decreasing the validity of results for both lift and moment. The doublet-lattice results for phase angle agree well with both CFD and test data except for in supersonic regions and cases with high reduced frequency. Linear theory predicts too small a phase lag in supersonic regions as expected because linear potential theory is not valid in regions where compressibility has a significant influence.

Using the results of our study, we are able to see that CFD is significantly better than the DLM for predicting control surface aerodynamics. As expected, the results from the CFD analysis are clearly in better agreement with the test data than are the results from linear potential theory. Because of better agreement with test data for the pressure magnitude on the flap, we can conclude that CFD analysis will consistently give more accurate hinge moment results. The phase shift due to local supersonic regions is captured excellently by the CFD analysis, which provides an excellent description of this flow behavior that cannot be accounted for by linear potential theory corrected by steady test data. This improved accuracy requires significantly more computer power than the linear solutions, but because the computations reported in this paper were all made on desktop workstations, we may yet see unsteady CFD simulations usurping the role of traditional linear potential unsteady aerodynamics tools in the aircraft design and certification processes.

References

[1]Rodden, W. P., Taylor, P. F., and McIntosh, S. C., Jr., "Further Refinements of the Nonplanar Aspects of the Subsonic Doublet-Lattice Lifting Surface Method," International Council of the Aeronautical Sciences, Paper 96-2.8.2, Sept. 1996.

[2]Rumsey, C., Sanetrik, M., Biedron, R., Melson, N., and Parlette, E., "Efficiency and Accuracy of Time-Accurate Turbulent Navier–Stokes Computations," *Computers and Fluids*, Vol. 25, No. 2, 1996, pp. 217–236.

[3]Scott, R. C., Hoadley, S. T., and Wiseman, C. D., "The Benchmark Active Controls Technology Model Aerodynamic Data," AIAA Paper 97-0829, Jan. 1997.

[4]Bartels, R., and Schuster, D., "Comparison of Two Navier–Stokes Methods with Benchmark Active Control Technology Experiments," *Journal of Guidance, Control, and Dynamics*, Vol. 23, No. 6, 2000, pp. 1094–1099.

[5]Schuster, D. M., Beran, P. S., and Huttsell, L. J., "Application of the ENS3DAE Euler/Navier–Stokes Aeroelastic Method," AGARD Rept. 822, Oct. 1997.

[6]Scott, R., Hoadley, S., Wieseman, C., and Durham, M., "Benchmark Active Controls Technology Model Aerodynamic Data," *Journal of Guidance, Control, and Dynamics*, Vol. 23, No. 5, 2000, pp. 914–921.

[7]Bennett, R., Scott, R., and Wieseman, C. D., "Computational Test Cases for the Benchmark Active Controls Model," *Journal of Guidance, Control, and Dynamics*, Vol. 23, No. 5, 2000, pp. 922–929.

[8]Presente, E., and Friedmann, P. P., "Active Control of Flutter in Compressible Flow and Its Aeroelastic Scaling," *Journal of Guidance, Control, and Dynamics*, Vol. 24, No. 1, 2000, pp. 167–175.

[9]Guillot, D., and Friedmann, P. P., "Fundamental Aeroservoelastic Study Combining Unsteady Computational Fluid Mechanics with Adaptive Control," *Journal of Guidance, Control, and Dynamics*, Vol. 23, No. 6, 2000, pp. 1117–1126.